

# OPTICAL PROPERTIES OF CO<sup>2+</sup>-DOPED ZNS NANOPARTICLES SYNTHESIZED USING REVERSE MICELLE METHOD

## Article history

Received  
17 December 2015  
Received in revised form  
3 March 2016  
Accepted  
20 Jun 2016

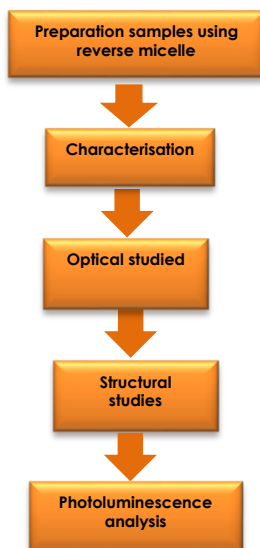
Rahizana Mohd Ibrahim<sup>a</sup>, Masturah Markom<sup>a\*</sup>, Kamal Firdausi Abd Razak<sup>b</sup>

\*Corresponding author  
masturahmarkom@ukm.edu.my

<sup>a</sup>Department of Chemical and Process Engineering, Faculty of Engineering and Built Environment, Universiti Kebangsaan Malaysia, 43600 Bangi, Malaysia

<sup>b</sup>Department of Petrochemical Engineering, Politeknik Tun Syed Nasir Syed Ismail, Hab Pendidikan Tinggi Pagoh, 84500 Muar, Johor, Malaysia

## Graphical abstract



## Abstract

Zinc sulfide is a luminescence materials with important application that exist either as a bulk material or in the form of nano crystal. Doped ZnS nanoparticles form a new class of luminescence materials and provide a new physics to control the particles size. This paper concerns detailed structural, spectroscopic and crystal field studies of ZnS nanoparticles, both pure and doped with CO<sup>2+</sup> ions that successfully synthesized at room temperature. Zn<sub>1-x</sub>Co<sub>x</sub>S (x =0.00,0.02,0.04,0.06,0.08 and 0.10) was prepared by reverse micelle method using sodium bis(2-ethylhexyl) sulfosuccinate (AOT) as surfactant. The effect of ion doping on the optical characterization, structure and morphology of ZnS:Co<sup>2+</sup> were investigated using ultraviolet-visible (UV-vis) spectroscopy, photoluminescence (PL) spectroscopy, X-ray diffraction (XRD), field-emission scanning electron microscopy (FESEM) and transmission electron microscopy (TEM). EDAX spectra confirmed the incorporation of ion dopants into ZnS crystal structure, and XRD results showed that ZnS:Co<sup>2+</sup> nanoparticles crystallized in a zinc blende structure. The particle size of all of samples ranged from 2 nm to 3 nm. In the PL emission, two peaks were observed at 460 and 608nm that a new peak for Co<sup>2+</sup> doped ZnS ever reported. The Co<sup>2+</sup> doped ZnS nanoparticles using reverse micelle method showed that there is considerable change in the photoluminescence spectra of the ZnS nanoparticle doped Co<sup>2+</sup>.

Keywords: Nanoparticles, ZnS:Co<sup>2+</sup>, reverse micelle method, quantum confinement effect, photoluminescence

© 2017 Penerbit UTM Press. All rights reserved

## 1.0 INTRODUCTION

ZnS is a wide band-gap semiconductor material (3.7eV) that currently is used commercially as a phosphor [1]. Recently, a branch of research studies has exploded in the area of luminescence characteristics of transition metal ion doped ZnS

semiconductor nanoparticles [2]. Most doped ZnS nanoparticles show a blue shift in optical spectra, which results from size quantization confinement [3]. Comprehensive studies have been conducted mainly on the optical properties of doped semiconductor nanoparticles [4, 5]. Doped ZnS semiconductors represent the possibility to form a new class of luminescence material due to the modification of

band structure by the formation of dopant levels within the ZnS band gap. During the chemical synthesis, impurity ions occupy the lattice sites and act as a trap site for electrons and holes. When the excited electron occurs, the relaxation of these photo-excited electrons to some surface states is followed by radiative decay, thus allowing luminescence in the visible region. This observation is interesting because it describes a different phenomenon from those of ZnS bulk materials.

For doped ZnS nanoparticles, the transformation of physical and chemical properties is dominated by the defect structure of the surface. Therefore, the tunable optical properties may be achieved by judiciously choosing the synthesis method, dopants, and their concentration. In addition, fabricating nanoparticles with a narrow size distribution will increase the surface area to volume ratio, thus increasing the specific chemical reactivity of the material. Various dopants such as Nickel, Ferum, and Manganese have been used to tune the optical properties of ZnS [6-8]. They have showed luminescence characterization in various regions, thus enhancing the excellent properties of ZnS. However, luminescence properties of Cobalt doped ZnS have rarely been researched. In addition,  $\text{Co}^{2+}$  has an ionic radius of 0.65 Å, which is smaller than that of  $\text{Zn}^{2+}$  (0.74 Å) given the possibility of the  $\text{Co}^{2+}$  ion easily replacing  $\text{Zn}^{2+}$  in the ZnS host lattice.

One of the most important methods of fabricating nanoparticles is through synthesis. A large variety of procedures have been developed for the synthesis of nanoparticles, such as co-precipitation, soft chemical method, sol-gel and solver thermal [9-12]. Among these various procedures for producing nanoparticles, the reverse micelle method is a considerable promising technique for preparing less agglomerated and more monodisperse nanoparticles [13]. In reverse micelle synthesis, oil is used as a template to restrict  $\text{H}_2\text{O}$  nanoreactors as reaction media. Consequently, during the chemical synthesis, excess particle growth can be avoided when it approaches that of an  $\text{H}_2\text{O}$  nanodroplet. This technique is an established method of synthesizing and stabilizing size-controlled nanoparticles. Sodium bis(2-ethylhexyl)sulfosuccinate (AOT) is the most commonly used surfactant in metal sulfide-nanoparticle synthesis by the reverse micelle method.

Therefore, this study will examine the synthesis of  $\text{Co}^{2+}$  doped ZnS as a prospective doping material in ZnS nanoparticles. Specifically, this study investigated the luminescence characteristic of nanoparticles  $\text{Zn}_{1-x}\text{Co}_x\text{S}$  ( $x = 0.00, 0.02, 0.04, 0.06, 0.08$  and  $0.10$ ) using the reverse micelle method. The optical properties, size, morphology, and structure of the resulting particles were investigated.

## 2.0 METHODOLOGY

Synthesis of  $\text{ZnS}:\text{Co}^{2+}$  nanoparticles was prepared in  $\text{H}_2\text{O}/\text{AOT}/n$ -heptane reverse micelle method using

precipitation technique. The selected W [( $\text{H}_2\text{O}$ )/( $\text{AOT}$ )] in molar ratio values was 7 in all preparation solution. In a typical procedure, reverse micelles that separately enclosed 0.5 M zinc acetate and 0.5 M nickel acetate (2%) were prepared. The two solutions were continuously stirred at 60 °C. Then, another reverse micelle of AOT that entrapped  $\text{Na}_2\text{S}$  solution was prepared.  $\text{Na}_2\text{S}$  solution was then added drop wise into the  $\text{Zn}^{2+}$  and  $\text{Co}^{2+}$  mixture with continuous stirring at 60 °C for 2 h. The resulting mixture was collected and allowed to stand for one day in an oven at a controlled temperature of 40°C for precipitation. After complete precipitation, the solution was centrifuged at 4000 rpm for 5 min. The precipitates were filtered and sequentially washed several times with ultrapure water and ethanol. Finally, the precipitates were dried in an oven at 40 °C for 8 h to remove  $\text{H}_2\text{O}$ , organic capping, and other by-products formed during the reaction. The same procedure was performed for the remaining four doping concentrations (4%, 6%, 8%, and 10%). The optical absorption spectra of the samples in ultrapure  $\text{H}_2\text{O}$  were measured using an AMBDA 35 ultraviolet (UV) spectrometer. Sample characterizations were performed using a NICOLET 6700 Fourier transform infrared (FT-IR) spectrometer. X-ray diffraction (XRD) patterns of the powdered samples were obtained using a D8 advance diffractometer from 20° to 80°. Crystal size was calculated using Scherrer equation  $(0.9\lambda)/(\beta\cos\theta)$  at full width at half-maximum (FWHM) of the XRD peaks. Nanoparticle morphology and size particles were determined using a field-emission scanning electron microscopy (FESEM) system (SUPRA 55VP) and transition electron microscopy (TEM) system (CM 12). Fluorescence measurements were performed using a PL SP920 spectrophotometer for optical characterization.

## 3.0 RESULTS AND DISCUSSION

The optical absorption of the samples are given in spectra Figure 1. The characteristic of absorption edge for undoped and  $\text{Co}^{2+}$  doped ZnS nanoparticles appear in the wavelength range of 240nm-340nm. The absorption edge of the samples exhibit large blueshift compared with bulk ZnS (345 nm). This blue shift due to the quantum confinement effect resulted from the small size of the particles formation [14]. From the figure, undoped ZnS showed two peak of absorption value which presented the formation of two group of particles size. While for  $\text{Co}^{2+}$  doped ZnS nanoparticles, the absorption graft exhibited a single absorption peak with a better narrow size distribution. However for doped ZnS, the absorption intensity vary with the change in the impurity ratio due to the effect of doped ions on the band gap structure. Therefore, particle size control was successful in the reverse

micelle system for doped ZnS using AOT as the capping agent. The highest absorption intensity was selected as the optimal value for further analysis.

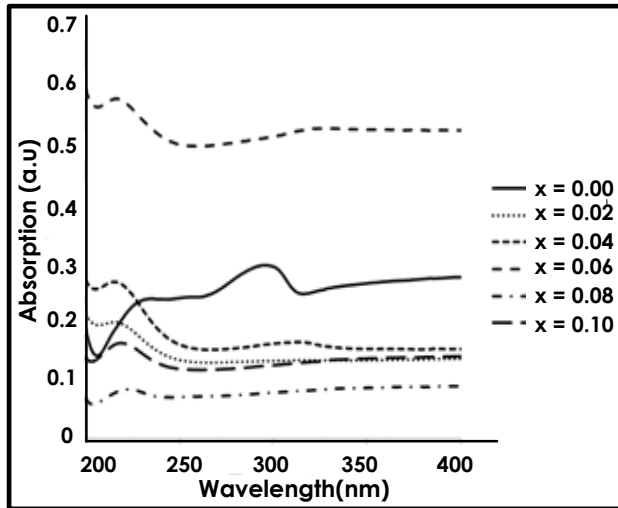


**Figure 1** UV-vis absorption spectra of  $Zn_{1-x}Co_xS$  ( $x=0.00, 0.02, 0.04, 0.06, 0.08, 0.10$ )

The UV-vis characteristic of absorption peaks can be used to determine the value of the optical band gap of the particles. The relation between absorption coefficients ( $\alpha$ ) and incident photon energy ( $h\nu$ ) can be written as [15].

$$\alpha = A(h\nu - E_g)^n / h\nu \quad (1)$$

Where  $A$  is a constant and  $E_g$  is the band gap of the material and the exponent  $n$  depends on the type of the transition. The value of " $n$ " are  $1/2$ ,  $2$ ,  $2/3$  and  $3$ , and these values corresponded with allowed direct, allowed indirect, forbidden direct and forbidden indirect transition, respectively. The transition value of undoped and  $Co^{2+}$  doped ZnS nanoparticles sample, is same as in the bulk sample. Then, the direct bandgap with  $n=1/2$  was obtained by extrapolating the straight portion of the plot of  $(\alpha h\nu)^2$  versus  $h\nu$  on  $h\nu$  axis at  $\alpha = 0$  as showed in Figure 2. In this sample, we chose to calculate the highest intensity of UV-vis absorption values for  $Co^{2+}$  doped ZnS. The values of optical band gap are 4.90 eV for undoped ZnS and 4.20 eV for 6%  $Co^{2+}$  doped ZnS. The changing in band gap value suggested that the occurrence of strong hybridization of s-p (in the ZnS host) and d (in the impurity) states [16]. From the bandgap value, the particles size was calculated using the theoretical effective mass approximation model formula [17]. The grain size of undoped and ZnS:Co(6%) was  $\sim 3$  nm, which was within the quantum confinement region.

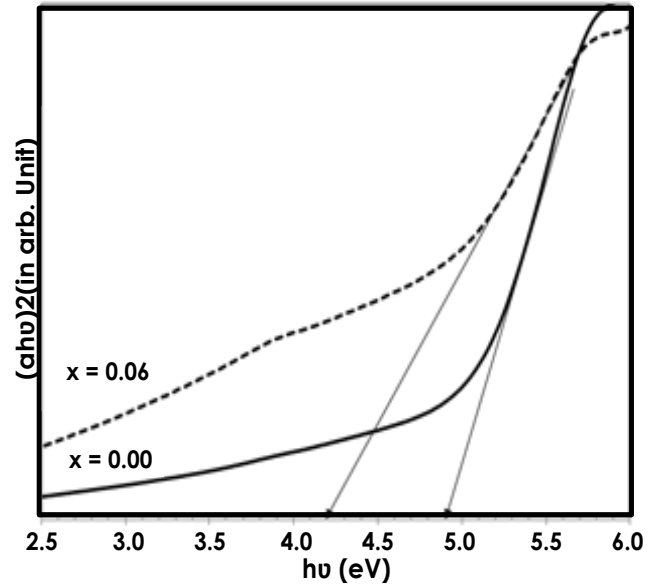


**Figure 2** Calculation of optical bandgap of (a) undoped ZnS (b) ZnS:Co(6%)

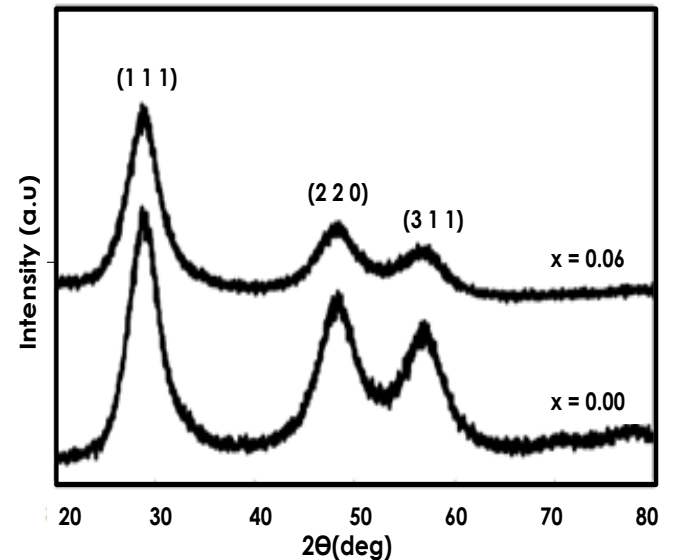


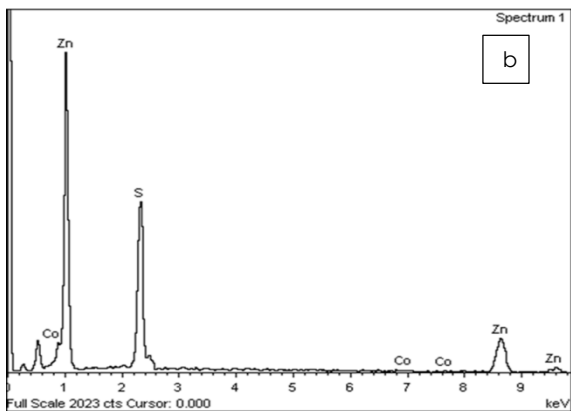
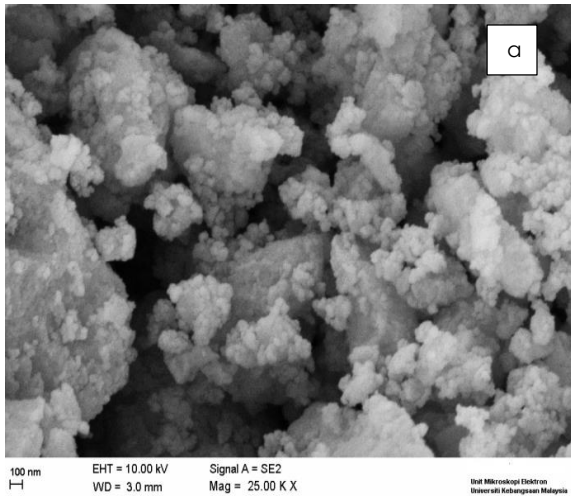
**Figure 3** X-ray diffraction (XRD) pattern of undoped ZnS and ZnS:Co(6%)

XRD pattern of the samples are showed in Figure 3 with no characteristic of impurity was observed. Three diffraction peaks at  $2\theta$  corresponding to reflections from (1 1 1), (2 2 0) and (3 1 1) planes of the cubic zinc blende phase and well matched with the standard cubic ZnS (JPSDS No. 05-0566). The broadening of XRD pattern indicated the nanocrystalline nature of the sample with slightly decrease in the intensity peak of  $Co^{2+}$  doped ZnS sample. The lattice contraction was believed to happen during the substitution of  $Co^{2+}$  ion with  $Zn^{2+}$  ion due to the differences in ionic radii. From

the XRD pattern, the average crystallize size were determined using the Debye Scherer formula [18].

$$D = k\lambda / \beta \cos\theta \quad (2)$$

Where D is the mean grain size, k is the constant shape factor ( $\sim 1$ ),  $\lambda$  is the wavelength of incident X-ray (1.54056 Å),  $\beta$  is the diffraction peak's FWHM and  $\theta$  is the Bragg's angle. The average crystallite sizes (D) was calculated by using the Eq.(2) from the most intense peak and tabulated in Table 1.



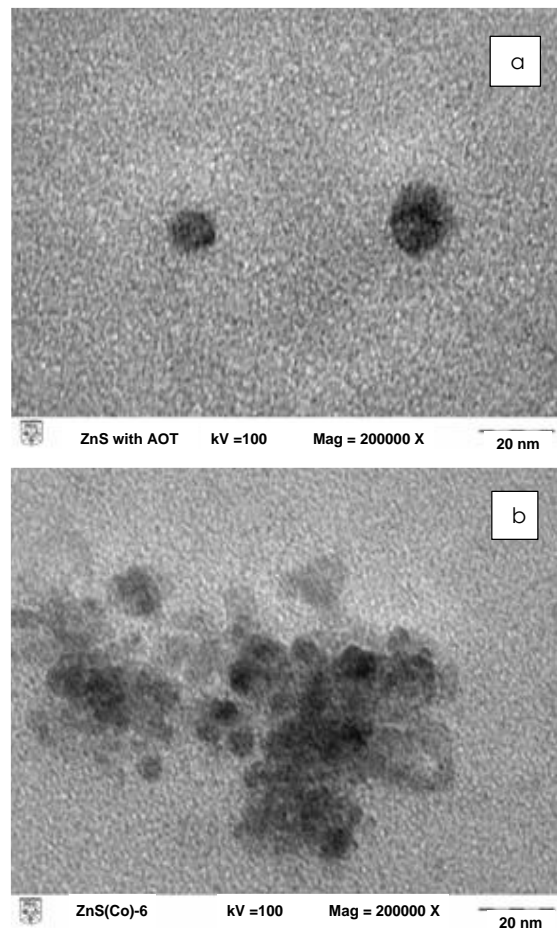
**Figure 4** (a) Field emission scanning electron microscope (FESEM) image of ZnS:Co(6%) (b) EDAX spectra of ZnS:Co(6%) sample

Figure 4(a) and (b) shows the FESEM image and EDAX spectra of ZnS:Co(6%) respectively. FESEM and EDAX spectra of ZnS:Co(6%) nanoparticles has been published [19]. From the FESEM image, the formation of  $\text{Co}^{2+}$ -doped ZnS nanoparticles is clearly observed. However, the actual size of nanoparticle cannot be measured due to the limitation in the resolution of the FESEM instrument. The EDAX spectrum confirmed the present of  $\text{Co}^{2+}$  ion in a ZnS nanoparticles structure. Therefore, the use of TEM instrument is necessary to obtain the particles size. Figures 5(a) and 5(b) shows the TEM image of ZnS and ZnS:Co(6%) with the mean

particle size obtained from the TEM analysis are summarize in Table 1.

**Table 1** Particle size and band gap as calculated from XRD, TEM and UV-vis absorption analysis

Sample	XRD (nm)	TEM (nm)	Band gap from UV(eV)	Particle size from UV(nm)
ZnS	2.53	6.18	4.9	3.24
ZnS:Co(6%)	2.39	7.15	4.2	2.72



**Figure 5** Transition electron microscope (TEM) micrograph of (a) ZnS and (b) ZnS:Co(6%)

Different group of researcher have study the PL characteristic of  $\text{Co}^{2+}$  doped ZnS. Previously, Sarkar *et al.* [20] reported that the PL emission intensity of ZnS:Co is  $\sim 35$  times greater than that of undoped ZnS at the same peak. Poornaprakash *et al.* [21] also reported that PL intensity is enhanced using  $\text{Co}^{2+}$  ion as dopant at the same peak of undoped ZnS. Yang *et al.* [22] reported that the emission wavelength is similar to that of ZnS, but the fluorescence intensity of  $\text{Co}^{2+}$ -doped ZnS is enhanced five times greater than that of ZnS.

However, Wensheng *et al.* [23] reported that  $\text{Co}^{2+}$ -doped ZnS showed the same emission as  $\text{Mn}^{2+}$ -doped ZnS with the emission peak of  $\text{Co}^{2+}$ -doped ZnS nanoparticles occurred at 430 and 572 nm. Therefore, these researchers supported the probability of  $\text{Co}^{2+}$ -doped ZnS appearing in the orange emission region. According to the presented results,  $\text{Co}^{2+}$  acted as a sensitizing agent in appropriate doping ratio. The fluorescence efficiency of the Co-doped ZnS samples are better than undoped ZnS due to the enhancement of the radiative recombination process.

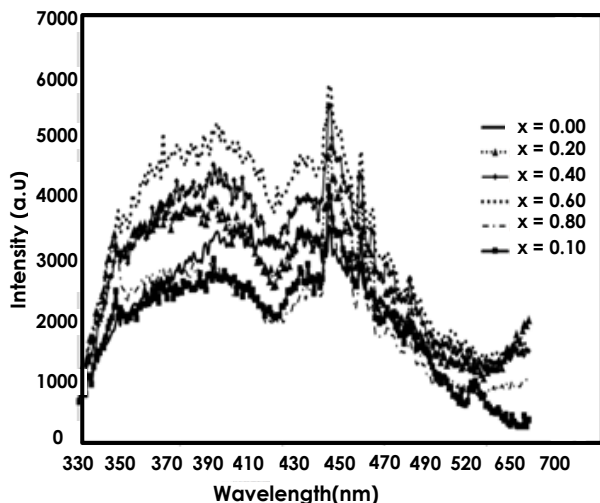


**Figure 6** Photoluminescence spectrum of  $\text{Zn}_{1-x}\text{Co}_x\text{S}$  as ( $x = 0.00, 0.02, 0.04, 0.06, 0.08, 0.10$ )

The optical absorption of undoped and different ratio of  $\text{Co}^{2+}$  doped ZnS nanoparticles have been analyzed. Figure 6 shows an identical PL spectra for all samples of  $\text{Co}^{2+}$  doped ZnS, at a 310 nm excitation wavelength. It is observed that all samples emitted a blue emission band centered at 400 nm with different intensity. The relative intensities of each of these bands varied with the change in doping ratio. As the  $\text{Co}^{2+}$  ratio increased up to  $x = 0.06$ , the PL intensity dramatically decreased. The different in PL intensity were mainly due to concentration quenching that attributed to the energy migration between the  $\text{Co}^{2+}$  pairs. Therefore, it is notable that the concentration quenching has been mainly attributed to the migration of the excitation energy between  $\text{Co}^{2+}$  ion pairs in the case of  $\text{Co}^{2+}$  doping. However, only  $\text{Co}^{2+}$  doped ZnS samples showed emission at visible region with multiple peaks at 440nm, 460nm and 608nm. The presence of multiple peaks indicated the involvement of different PL centers in the radiation process. Interestingly, the characteristic of orange emission center of  $\text{Co}^{2+}$  ion doped ZnS was something new. Our results showed the appearance of an emission peak at a longer wavelength, which provided a new finding for the luminescence center of  $\text{Co}^{2+}$ -doped ZnS. Therefore, in reverse micelle synthesis, the incorporation of ion  $\text{Co}^{2+}$  have attributed to

modification coordination of  $\text{Co}^{2+}$  in ZnS nanoparticles.

This finding revealed that particle growth was controlled by the entire reverse micelle system. Therefore, PL spectra provided an excellence method of studying the formation of  $\text{Co}^{2+}$  doped ZnS nanoparticles during chemical synthesis.

## 4.0 CONCLUSION

$\text{Co}^{2+}$  doped ZnS has been successfully synthesized using reverse micelle method. The average particle size of the samples ranges from 2.5 nm to 3.5 nm, which indicated the strong quantum size effect. The PL spectra of samples showed that  $\text{Co}^{2+}$  ion exhibited different degrees of incorporation into the ZnS host structure. The particles exhibited the characteristic orange emission (608 nm) which provide a new finding for ZnS emission spectra. Therefore, the enhancement of fluorescence efficiency in  $\text{Co}^{2+}$  doped ZnS nanoparticle is very important in the research of luminescence materials. Thus, PL spectra provided an excellence method of studying the formation of  $\text{Co}^{2+}$  doped ZnS nanoparticles during chemical synthesis.

## Acknowledgement

The authors are grateful to the financially supported by Universiti Kebangsaan Malaysia which under Project FRGS/2/2013/TK05/UKM/02/2.

## References

- [1] Karen Grieve, Paul Mulvaney, Franz Grieser. 2000. Synthesis and Electronic Properties of Semiconductor Nanoparticles/Quantum Dot. *Current Opinion in Colloid & Interface Science*. 5: 168-17.
- [2] Wei Chen, Jin Z. Zhang, Alan G. Joly. 2004. Optical Properties and Potential Applications of Doped Semiconductor Nanoparticles. *J. Nanosci. Nanotech.* 4: 919-947.
- [3] He Hu, Weihua Zhang 2006. Synthesis and Properties of Transition Metals and Rare-earth Metals doped ZnS Nanoparticles. *Optical Materials*. 28: 536-550.
- [4] Xiaosheng Fang, Tianyou Zhai, Ujjal K. Gautam, Liang Li, Limin Wua, Yoshio Bando, Dmitri Golberg. 2011. ZnS Nanostructure; from Synthesis to Application. *Progress in Materials Science*. 56: 175-287.
- [5] C. S. Pathak, M. K. Mandal, V. Agarwala. 2013. Optical Properties of Undoped and Cobalt Doped ZnS nanophosphor. *Materials Science in Semiconductor Processing*. 16: 467-471.
- [6] G. Murugadoss, M. Rajesh Kumar. 2014. Synthesis and Optical Properties of Monodispersed  $\text{Ni}^{2+}$ -doped ZnS Nanoparticles. *Applied Nanoscience*. 4: 67-75.
- [7] S. Sambasivama, D. Paul Joseph, D. Raja Reddy, B. K. Reddy, C. K. Jayasankar. 2008. Synthesis and Characterization of Thiophenol Passivated Fe-doped ZnS Nanoparticles. *Materials Science and Engineering B*. 150: 125-12.
- [8] H. C. Warad, S. C. Ghosh, B. Hemtanon, C. Thanachayanont, J. Dutta. 2005. Luminescent Nanoparticles of Mn doped ZnS Passivated with Sodium

- Hexamethaphosphate. *Science and Technology of Advanced Materials*. 6: 296-301.
- [9] Remi Beaulac, Paul I. Archer, Danial R. Gamelin .2008. Luminescence in Colloidal Mn<sup>2+</sup>-doped Semiconductor Nanocrystal. *Journal of Solid State Chemistry*. 181: 1582-1589.
- [10] Qitao Zhao, Lisong Hou, Ruian Huang. 2003. Synthesis of ZnS Nanorods by a Surfactant-assisted Soft Chemistry Method. *Inorganic Chemistry Communications*. 6: 971-973.
- [11] M. M. Biggs, O. M. Ntwaeaborwa, J. J. Terblans, H. C. Swart. 2009. Characterization and Luminescent Properties of SiO<sub>2</sub>:ZnS:Mn<sup>2+</sup> and ZnS:Mn<sup>2+</sup> Nanophosphors Synthesized by a Sol-gel Method. *Physica B*. 404: 4470-4475.
- [12] Daixun Jiang, Lixin Cao , Ge Su, Hua Qu, Dake Sun. 2007. Luminescence Enhancement of Mn doped ZnS Nanocrystals. *Applied Surface Science*. 253: 9330-9335.
- [13] Jun Zhang, Lingdong Sun, Chunsheng Liao, Chunhua Yan. 2002. Size Control and Photoluminescence Enhancement of CdS Nanoparticles Prepared via Reverse Micelle Method. *Solid State Communications*. 124: 45-48.
- [14] R.Saravanan 2010.Growth and Local Structure Analysis of ZnS Nanoparticles. *Physic B*. 405: 3700-3703.
- [15] Alessia Le Donne, Sourav Kanti Jana, Sangam Banerjee, Sukumar Basu, Simona Binetti. 2013. Optimized Luminescence Properties of Mn doped ZnS Nanoparticles for Photovoltaic Applications. *Journal of Applied Physics*. 113: 014903.
- [16] C. S. Tiwary, P.Kumbhakar, A. K. Mitr, K. Chattopadhyay. 2009. Synthesis of Wurtzite-Phase ZnS Nanocrystal and Its Optical Properties. *Journal of Luminescence*. 129: 1366-1370.
- [17] G. Murugadoss, B. Rajamannan, V. Ramasamy, G. Viruthalagiri. 2009. Synthesis and Characterization of Mn<sup>2+</sup> doped ZnS Luminescent Nanocrystal. *Journal of Ovonic Research*. 107-116.
- [18] H. C. Warad, S. C. Ghosh, B. Hemtanon, C. Thanachayanont, J. Dutta. 2005. Luminescent Nanoparticles of Mn doped ZnS Passivated with Sodium Hexamethaphosphate. *Science and Technology of Advanced Materials*. 6: 296-301.
- [19] Rahizana Mohd Ibrahim, Masturah Markom, Huda Abdullah, Optical Properties of Ni<sup>2+</sup>, Co<sup>2+</sup>, and Mn<sup>2+</sup>-doped ZnS Nanoparticles Synthesized Using Reverse MicelleMethod. *ECS Journal of Solid State Science and Technology*. 4(2): R31-R37.
- [20] R. Sarkar, C. S. Tiwary, P. Kumbhakar, A. K. Mitra. 2009. Enhanced Visible Light Emission from Co<sup>2+</sup> doped ZnS Nanoparticles. *Physica B*. 404: 3855-3858.
- [21] B. Poornaprakash, D. Amaranatha Reddy, G. Murali, N. Madhusudhana Rao, R. P. Vijayalakshmi, B. K. Reddy. 2013. Composition Dependent Room Temperature Ferromagnetism and PL Intensity of Cobalt Doped ZnS Nanoparticles. *Journal of Alloys and Compounds*. 577: 79-85.
- [22] Ping Yang, Mengkai Lü, Guangjun Zhou, DuoRong Yuan Dong Xu. 2001. Photoluminescence Characteristics of ZnS Nanocrystallites co-doped with Co<sup>2+</sup> and Cu<sup>2+</sup>. *Inorganic Chemistry Communications*. 4: 734-737.
- [23] Wen-sheng Zou, Jun-qin Qiao, Xin Hu, Xin Ge, Hong-zhen Lian. 2011. Synthesis in Aqueous solution and characterisation of a New Cobalt-doped ZnS Quantum Dot As a Hybrid Ratiometric chemosensor. *Analytica Chimica Acta*. 708: 134-140.